Supporting Information

Molecular Composition of Fresh and Aged Aerosols from Residential Wood Combustion and Gasoline Car with Modern Emission Mitigation Technology

Eric Schneider[a,b], Hendryk Czech[a,c,*], Anni Hartikainen[d], Helly J. Hansen[a], Nadine Gawlitta[c], Mika Ihalainen[d], Pasi Yli-Pirilä[d], Markus Somero[d], Miika Kortelainen[d], Juho Louhisalmi[d], Jürgen Orasche[c], Zheng Fang[e], Yinon Rudich[e], Olli Sippula[d,f], Christopher P. Rüger[a,b] and Ralf Zimmermann[a,b,c]

[a]Joint Mass Spectrometry Centre, Department of Analytical and Technical Chemistry, University of Rostock, Rostock, Germany

[b]Department Life, Light & Matter (LL&M), University of Rostock, Rostock, Germany

[c]Joint Mass Spectrometry Centre, Cooperation Group "Comprehensive Molecular Analytics" (CMA), Helmholtz Centre Munich, Munich, Germany

[d]Department of Environmental and Biological Sciences, University of Eastern Finland, Kuopio, Finland

[e]Department of Earth and Planetary Sciences, Weizmann Institute of Science, Rehovot, Israel

[f]Department of Chemistry, University of Eastern Finland, Joensuu, Finland

Corresponding author email: Hendryk Czech (hendryk.czech@uni-rostock.de)

Table of contents

Section S1. Calculation of molecular properties

Formulae applied for the calculation of double bond equivalents (DBE), aromaticity index (AI, modified for high oxygen content),[1,2] saturation vapour pressure (C*, Table S1).[3] Calculations are based on the assigned neutral sum formulae $C_cH_hN_nO_oS_s$.

$$DBE = c - \frac{h}{2} + \frac{n}{2} + 1 \quad (1)$$

$$AI_{mod} = \frac{1+c-0.5\,o-s-0.5\,h}{c-0.5\,o-s-n} \quad (2)$$

$AI_{mod} > 0.5$ indicates aromatic structures and $AI_{mod} > 0.67$ indicates condensed aromatic structures.

$$\log_{10} C^* = (n_c^0 - c)b_c - ob_o - 2\,\frac{c\,o}{c+o} b_{co} - nb_n - sb_s \quad (3)$$

Organic aerosol compounds can be classified into five groups, based on their saturation vapor pressure (C^*): volatile organic compounds (VOC; $C^* > 3\times10^6$ µg m^{-3}), intermediate volatility OC (IVOC; $300 < C^* < 3\times10^6$ µg m^{-3}), semi volatile OC (SVOC; $0.3 < C^* < 300$ µg m^{-3}), low-volatile OC (LVOC; $3\times10^{-4} < C^* < 0.3$ µg m^{-3}), and extremely low-volatile OC (ELVOC; $C^* < 3\times10^{-4}$ µg m^{-3}). [4,5]

Table S1: Compound classes and their respective n^0_C and b values from Li et al. [3] obtained by least-squares optimization using compounds from the NCI database.

Compound class	n^0_C	b_c	b_o	b_{co}	b_n	b_s
CH	23.8	0.4861				
CHO	22.66	0.4481	1.656	−0.7790		
CHN	24.59	0.4066			0.9619	
CHNO	24.13	0.3667	0.7732	−0.07790	1.114	
CHOS	24.06	0.3637	1.327	−0.3988		0.7579
CHNOS	28.5	0.3848	1.011	0.2921	1.053	1.316

Table S2: Absolute number of assigned elemental compositions in each compound class.

ionization	sample	number of assigned compounds					
		CH	CHO	CHNO	CHOS	CHNOS	CHN
APPI	Car fresh	56	513	51	0	0	0
	Car short	26	450	1161	0	0	0
	Car medium	79	800	2861	5	0	18
	Wood fresh	156	750	207	0	0	22
	Wood short	109	1160	848	0	0	10
	Wood medium	63	1328	1426	0	0	7
	ESP Wood fresh	181	1031	466	0	0	40
	ESP Wood short	67	844	695	0	0	8
ESI negative	Car fresh	0	214	97	46	9	0
	Car short	0	361	1078	6	109	0
	Car medium	0	621	2227	120	390	0
	Wood fresh	0	666	272	93	18	0
	Wood short	0	962	1469	123	60	0
	Wood medium	0	942	940	158	10	0
	ESP Wood fresh	0	551	543	128	55	0
	ESP Wood short	0	943	1520	112	128	0
ESI positive	Car fresh	0	580	202	0	0	15
	Car short	0	388	1328	0	0	5
	Car medium	30	643	401	0	0	51
	Wood fresh	19	318	112	0	0	5
	Wood short	8	867	771	0	0	26
	Wood medium	0	844	857	0	0	13
	ESP Wood fresh	21	718	785	0	0	54
	ESP Wood short	0	718	916	0	0	20

ESP: electrostatic precipitator

Table S3: Absolute intensity of assigned elemental compositions in each compound class.

ionization	sample	intensity of assigned compounds [a.u.]						
		CH	CHO	CHNO	CHOS	CHNOS	CHN	total
APPI	Car fresh	1.20E+09	6.55E+09	6.93E+08	0	0	0	8.44E+09
	Car short	1.33E+08	1.58E+09	4.70E+09	0	0	0	6.41E+09
	Car medium	2.39E+08	3.74E+09	2.29E+10	3.98E+07	0	6.88E+07	2.71E+10
	Wood fresh	2.94E+09	1.85E+10	8.96E+08	0	0	1.52E+08	2.25E+10
	Wood short	1.30E+09	1.59E+10	4.19E+09	0	0	4.71E+07	2.15E+10
	Wood medium	3.86E+08	1.90E+10	1.04E+10	0	0	2.65E+07	2.98E+10
	ESP Wood fresh	5.28E+09	2.81E+10	2.36E+09	0	0	2.33E+08	3.60E+10
	ESP Wood short	2.71E+08	7.11E+09	2.58E+09	0	0	2.24E+07	9.99E+09
ESI negative	Car fresh	0	5.07E+09	5.49E+08	1.34E+09	4.50E+07	0	7.00E+09
	Car short	0	1.72E+09	4.86E+09	1.02E+07	2.98E+08	0	6.89E+09
	Car medium	0	5.48E+09	1.60E+10	3.80E+08	1.28E+09	0	2.31E+10
	Wood fresh	0	5.10E+09	1.00E+09	6.48E+08	9.96E+07	0	6.86E+09
	Wood short	0	7.47E+09	9.23E+09	4.15E+08	1.76E+08	0	1.73E+10
	Wood medium	0	6.80E+09	4.47E+09	4.83E+08	2.01E+07	0	1.18E+10
	ESP Wood fresh	0	1.40E+10	2.24E+09	7.86E+08	1.95E+08	0	1.72E+10
	ESP Wood short	0	6.25E+09	9.01E+09	3.91E+08	4.18E+08	0	1.61E+10
ESI positive	Car fresh	0	3.55E+09	1.21E+09	0	0	5.67E+07	4.81E+09
	Car short	0	1.27E+09	5.02E+09	0	0	1.11E+07	6.30E+09
	Car medium	4.76E+07	2.39E+09	1.02E+09	0	0	1.67E+08	3.63E+09
	Wood fresh	4.75E+07	1.34E+09	4.92E+08	0	0	5.48E+07	1.94E+09
	Wood short	4.99E+07	3.66E+09	3.76E+09	0	0	9.92E+07	7.57E+09
	Wood medium	0	3.12E+09	4.61E+09	0	0	4.42E+07	7.78E+09
	ESP Wood fresh	6.41E+07	4.29E+09	4.56E+09	0	0	2.34E+08	9.15E+09
	ESP Wood short	0	2.38E+09	4.23E+09	0	0	6.10E+07	6.67E+09

ESP: electrostatic precipitator

Table S4: Arithmetic mean of parameters calculated from the elemental composition for each dataset.

ionization	sample	number	OS_C	DBE	AI_{mod}	H/C	O/C	O/N	C	H	N	O	m/z
APPI	Car fresh	620	-1.12	6.9	0.31	1.40	0.15	2.86	21.8	31.8	0.1	2.7	338.6
	Car short	1637	-0.59	5.9	0.22	1.39	0.41	4.11	14.8	20.9	1.1	5.0	296.3
	Car medium	3784	-0.55	6.3	0.21	1.39	0.43	4.14	15.5	21.8	1.4	5.7	320.8
	Wood fresh	1135	-0.62	12.9	0.59	0.87	0.15	2.51	21.1	18.8	0.2	2.3	313.5
	Wood short	2127	-0.42	12.5	0.55	0.91	0.26	4.66	20.0	17.6	0.4	4.1	331.1
	Wood medium	2824	-0.26	12.6	0.53	0.90	0.33	5.62	19.7	16.7	0.6	5.5	349.4
	ESP Wood fresh	1718	-0.64	13.5	0.57	0.90	0.15	2.88	22.3	19.9	0.3	2.6	333.7
	ESP Wood short	1614	-0.43	10.8	0.51	0.97	0.28	4.56	18.3	17.3	0.5	4.2	311.1
ESI negative	Car fresh	366	-1.34	3.1	0.07	1.84	0.25	3.76	20.6	37.4	0.3	4.6	367.2
	Car short	1554	0.21	6.0	0.12	1.32	0.77	6.47	12.6	16.6	1.3	9.2	334.9
	Car medium	3358	0.27	6.8	0.14	1.28	0.77	6.45	13.8	17.5	1.5	10.1	370.5
	Wood fresh	1055	-0.51	11.4	0.48	1.04	0.26	4.29	20.8	21.2	0.3	4.9	357.3
	Wood short	2614	0.27	10.9	0.43	0.91	0.59	7.70	16.7	14.3	0.8	8.8	367.7
	Wood medium	2050	0.48	9.7	0.36	0.95	0.72	9.31	15.4	14.0	0.5	10.1	370.9
	ESP Wood fresh	1282	-0.33	12.7	0.53	0.92	0.29	5.32	20.7	18.6	0.6	5.5	367.0
	ESP Wood short	2703	0.25	10.5	0.41	0.94	0.59	7.48	16.5	14.8	0.8	8.8	367.9
ESI positive	Car fresh	797	-1.33	3.7	0.11	1.77	0.23	2.93	18.7	32.4	0.3	3.7	340.2
	Car short	1721	-0.65	3.8	0.06	1.66	0.51	4.56	13.2	22.1	1.1	6.1	302.3
	Car medium	1125	-0.76	8.6	0.33	1.26	0.27	3.93	18.7	22.8	0.6	4.3	344.0
	Wood fresh	454	-0.49	12.3	0.57	0.90	0.22	4.76	19.7	17.1	0.3	3.5	333.5
	Wood short	1672	-0.44	9.6	0.45	1.06	0.32	4.01	16.6	16.5	0.5	4.5	305.4
	Wood medium	1714	-0.23	9.1	0.41	1.08	0.43	5.17	15.8	15.8	0.5	5.9	316.8
	ESP Wood fresh	1578	-0.61	10.7	0.46	1.07	0.25	3.71	19.1	19.5	0.7	4.0	341.6
	ESP Wood short	1654	-0.57	7.3	0.33	1.28	0.36	4.12	15.5	19.1	0.6	4.8	301.9

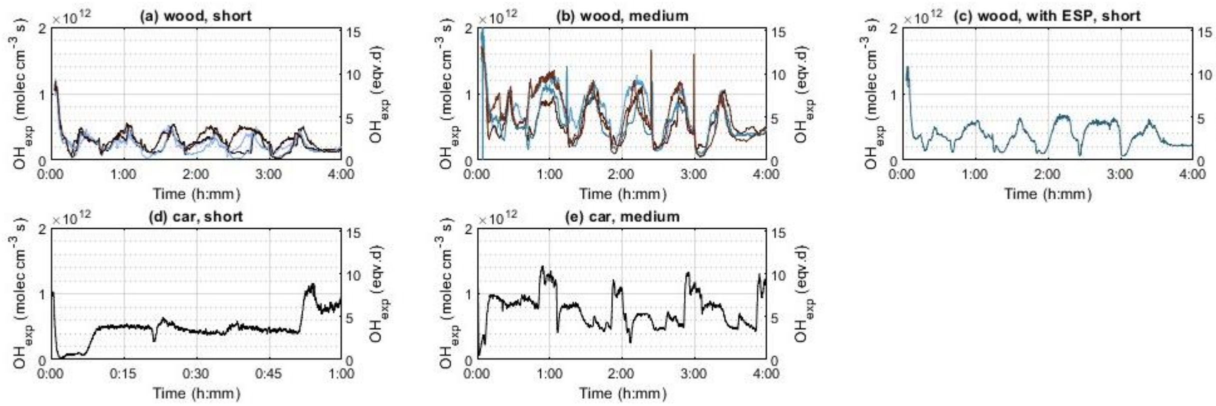

Figure S1: OH exposure during the experiments, assessed from the consumption of externally input d9-butanol. For the car experiments, d9-butanol was monitored only for one 1h cycle (short aging, d) experiment or for one 4 h experiment, consisting of four repetitive cycles (medium aging, e).

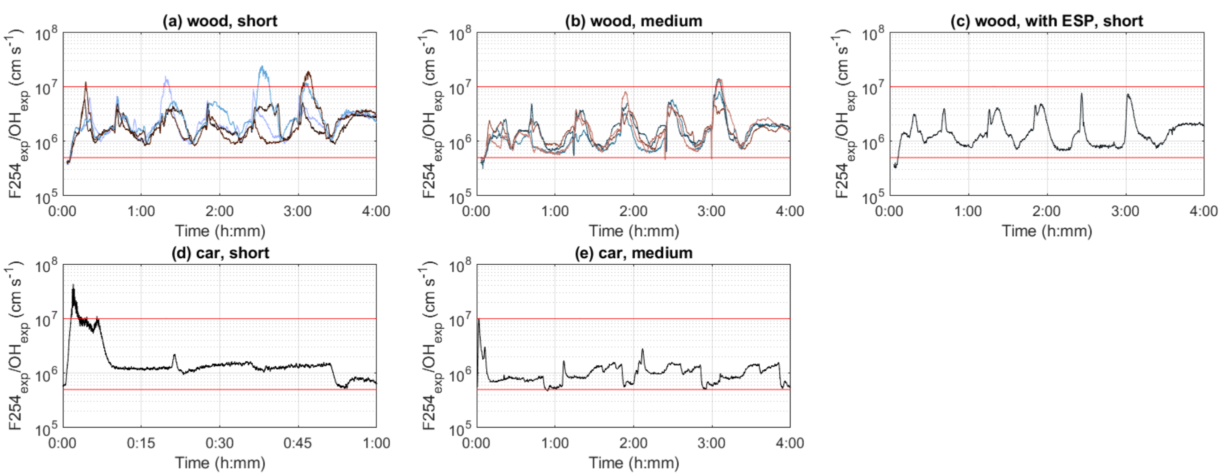

Figure S2: Ratio of photolysis ($F_{254,\ exp}$) to OH exposure (OH_{exp}) during the experiments. Ratios of 4×10^5 cm s^{-1} and 1×10^7 cm s^{-1} are shown as the lower limits for 'risky' and 'bad' oxidative flow reaction conditions, respectively, as defined by Peng and Jimenez.[6]

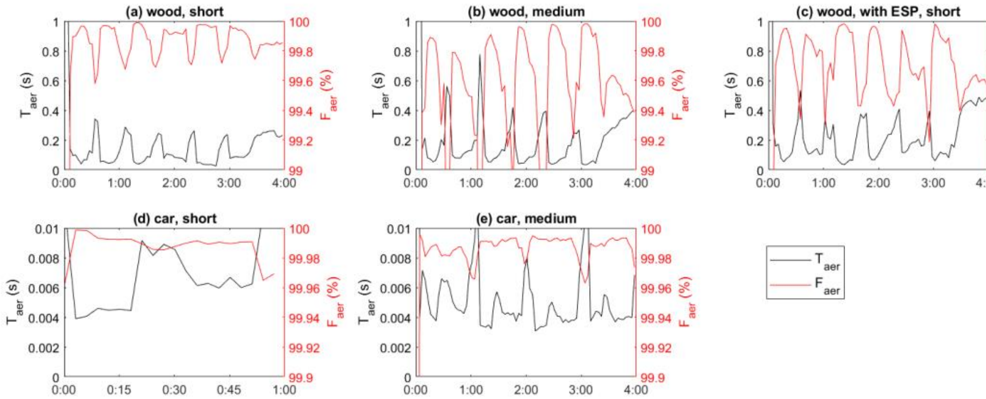

Figure S3: Examples of LVOC lifetimes regarding the particulate condensation sinks (T_{aer}) downstream the PEAR, and the fraction of LVOCs estimated to have condensed onto particles within their residence in the PEAR (F_{aer}) in short and medium aged wood combustion experiments (a and b, respectively), wood combustion with ESP (c), and in the short and medium aged car experiments (d and e, respectively). LVOC fates were modelled similarly to Hartikainen et al. and Palm et al. based on particle size distributions measured after the PEAR.[7,8]

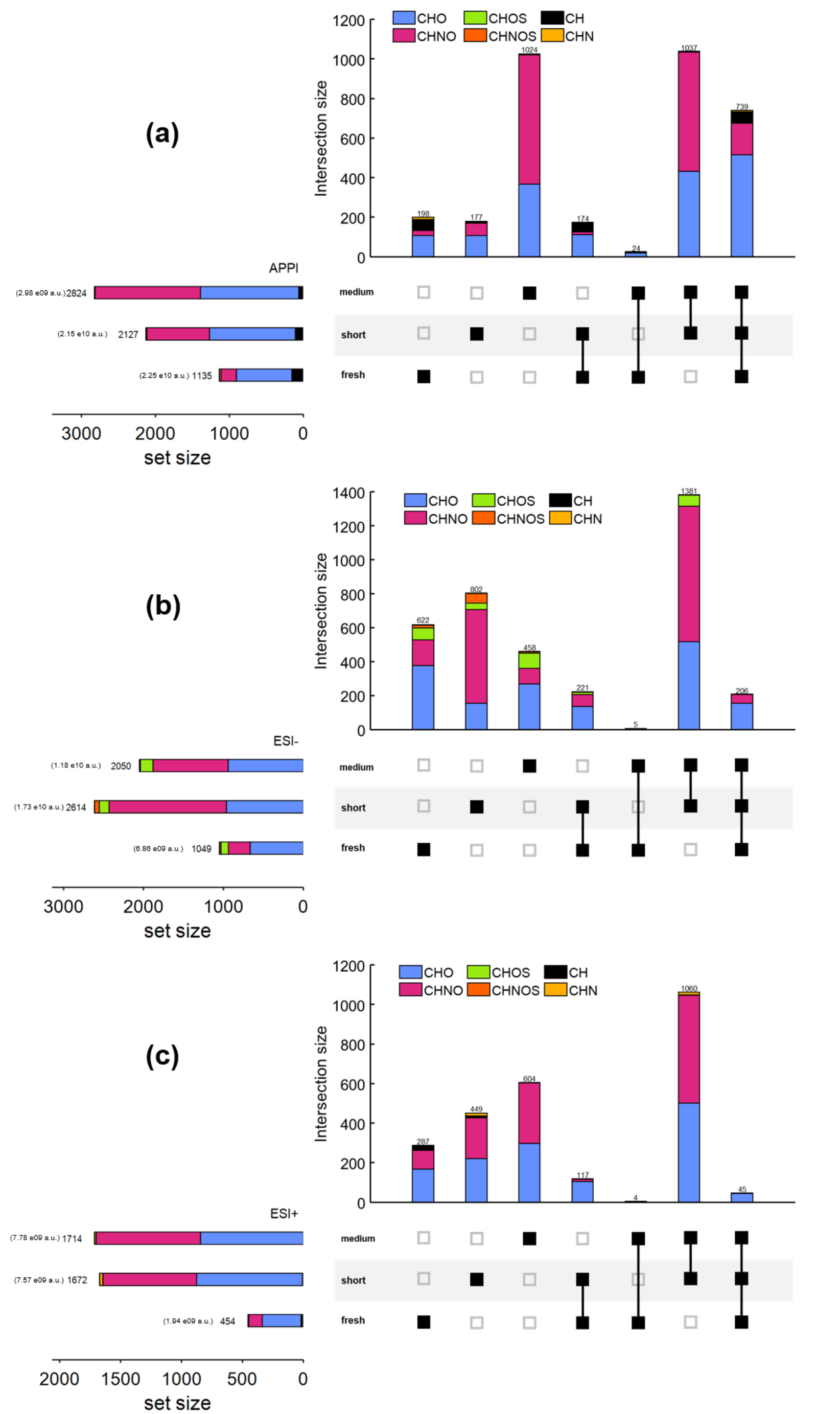

Figure S4: Upset plots of assigned elemental compositions from fresh, short aged and medium aged residential wood combustion emissions with indicated compound class, detected in **(a)** APPI **(b)** ESI- and **(c)** ESI+. Upset plots are used to visualize the number as well as chemical composition within each intersect of a Venn diagram. The black squares underneath each plot indicate which intersection of datasets is addressed by the respective bar. TIC (set size) is indicated in brackets behind the respective number of compounds in each dataset.

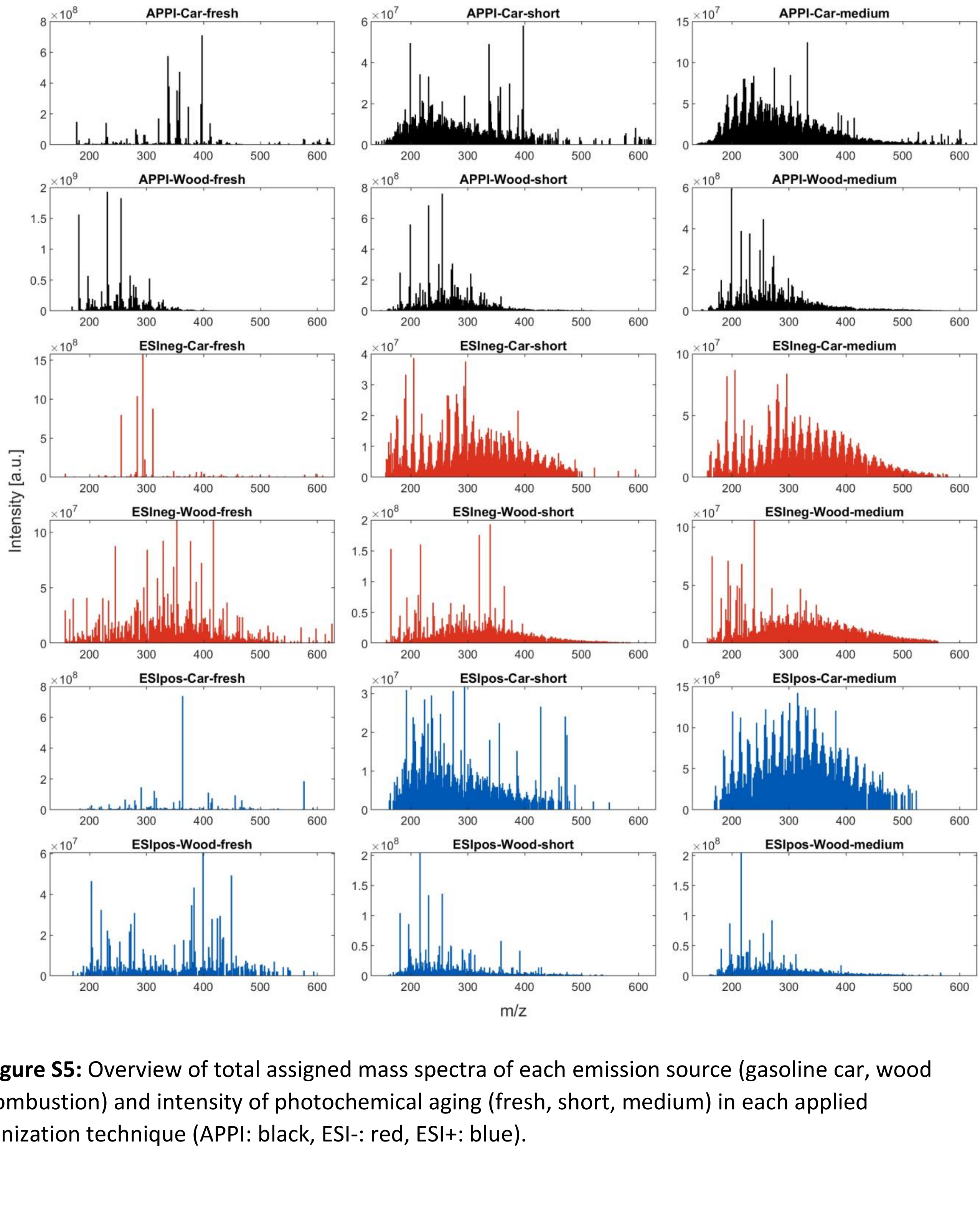

Figure S5: Overview of total assigned mass spectra of each emission source (gasoline car, wood combustion) and intensity of photochemical aging (fresh, short, medium) in each applied ionization technique (APPI: black, ESI-: red, ESI+: blue).

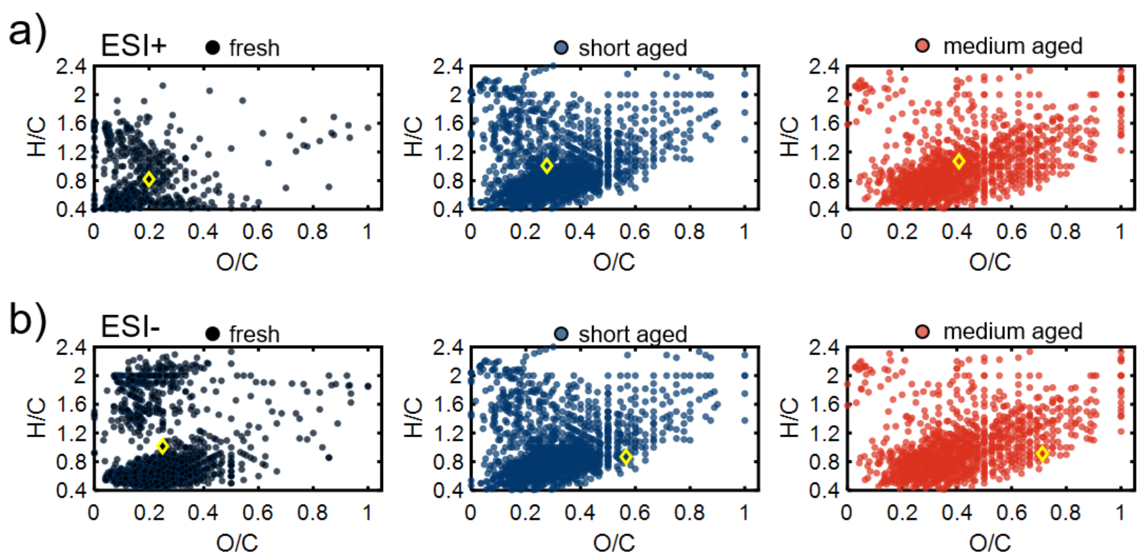

Figure S6: Van Krevelen diagrams of residential wood combustion emissions **(a)** ESI+ and (**b)** ESI- data with fresh organic aerosol indicated in black (left) and compounds newly formed during short aging (center) indicated in blue and compounds only formed during medium aging (right) displayed in red. The dot size indicates the number of oxygen atoms in the sum formula.

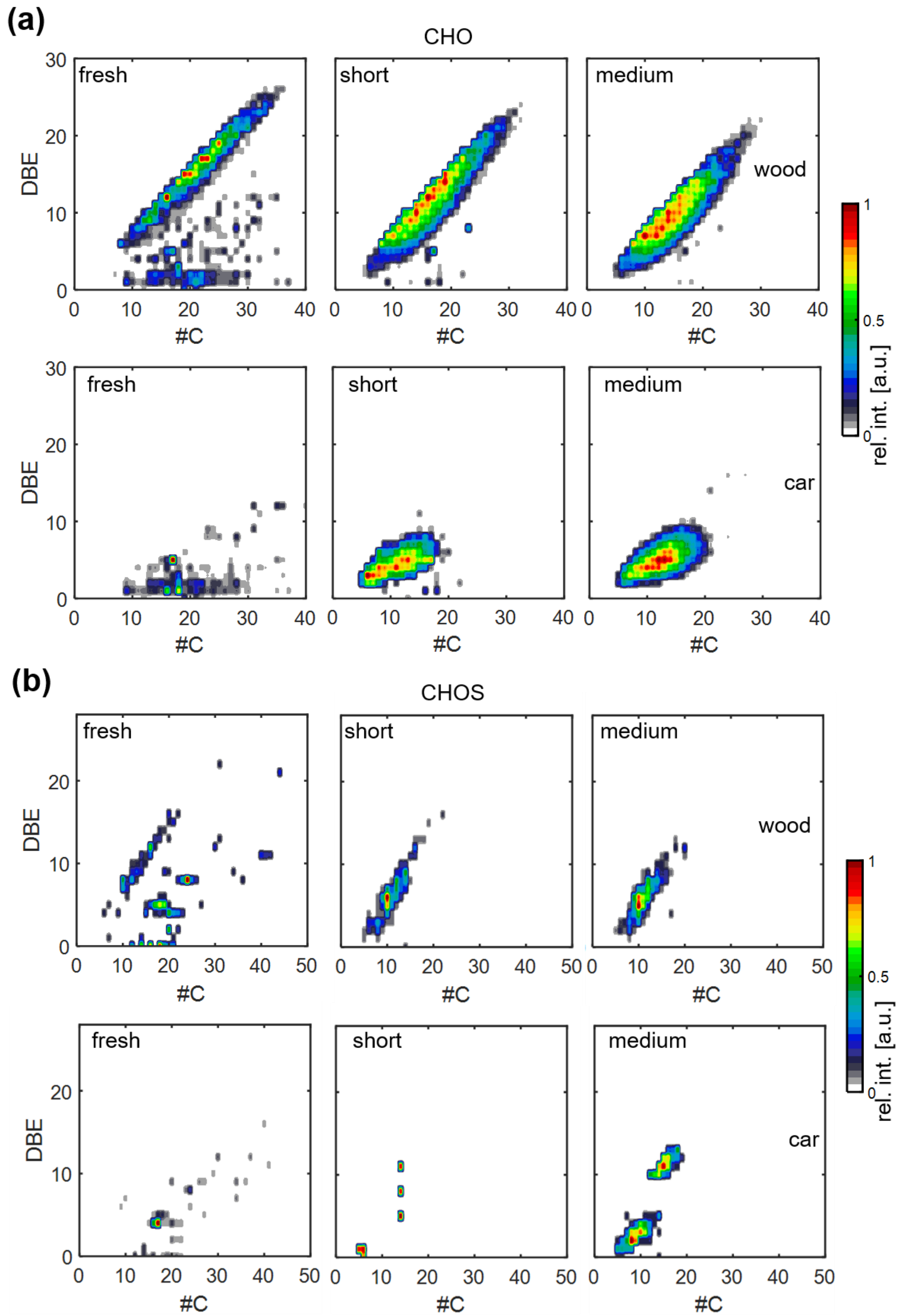

Figure S7: Contour plot of double bond equivalent (DBE) versus carbon number plot of the (a) CHO and (b) CHOS compound class in fresh, short aged and medium aged ESI- data of residential wood combustion emissions (top) and gasoline car emissions (bottom).

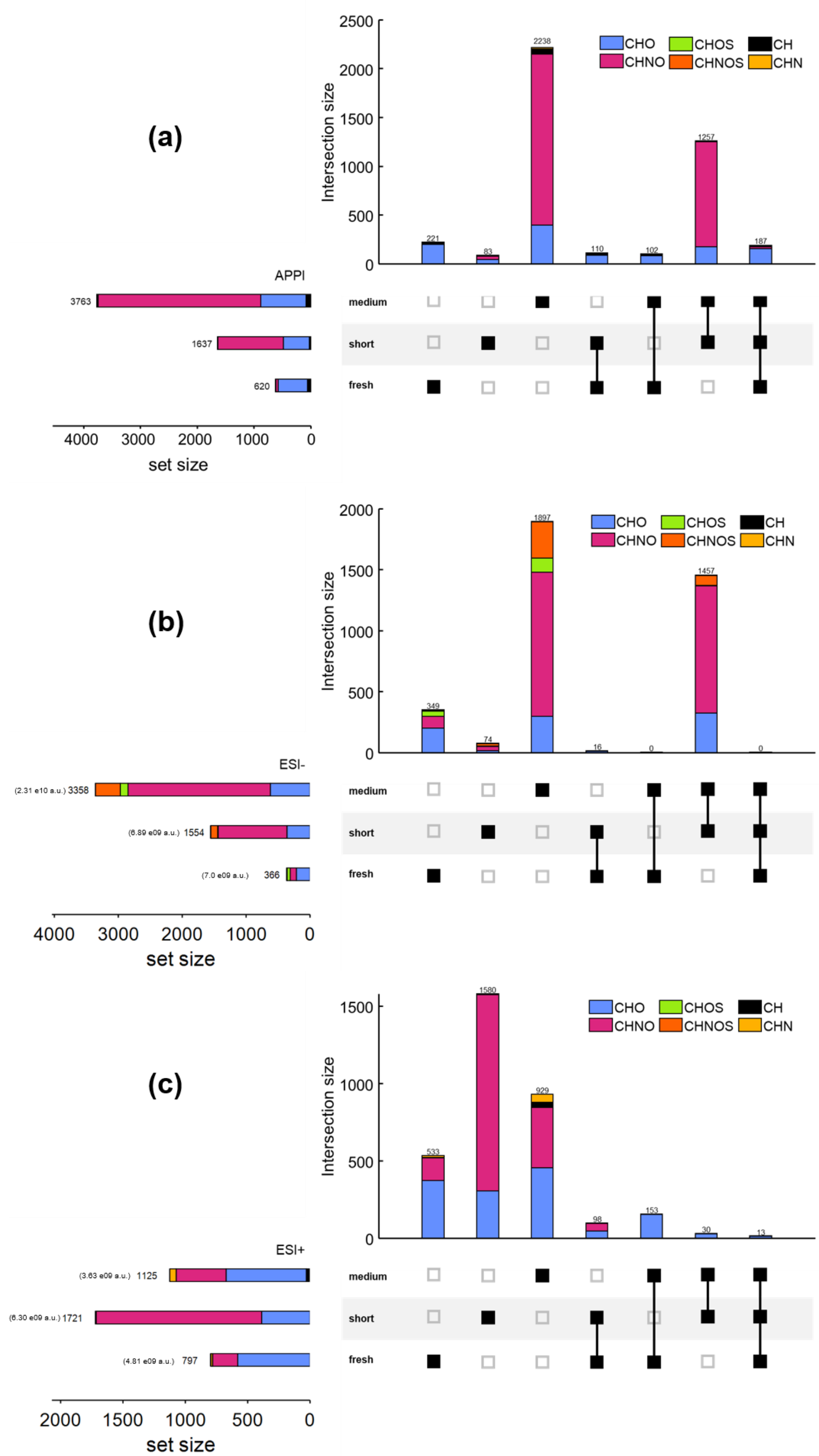

Figure S8: Upset plots of assigned elemental compositions from fresh and short aged residential wood combustion emissions with optional application of an electrostatic precipitator (ESP) and with indicated compound class, detected in **(a)** APPI **(b)** ESI- and **(c)** ESI+. TIC (set size) is indicated in brackets behind the respective number of compounds in each dataset.

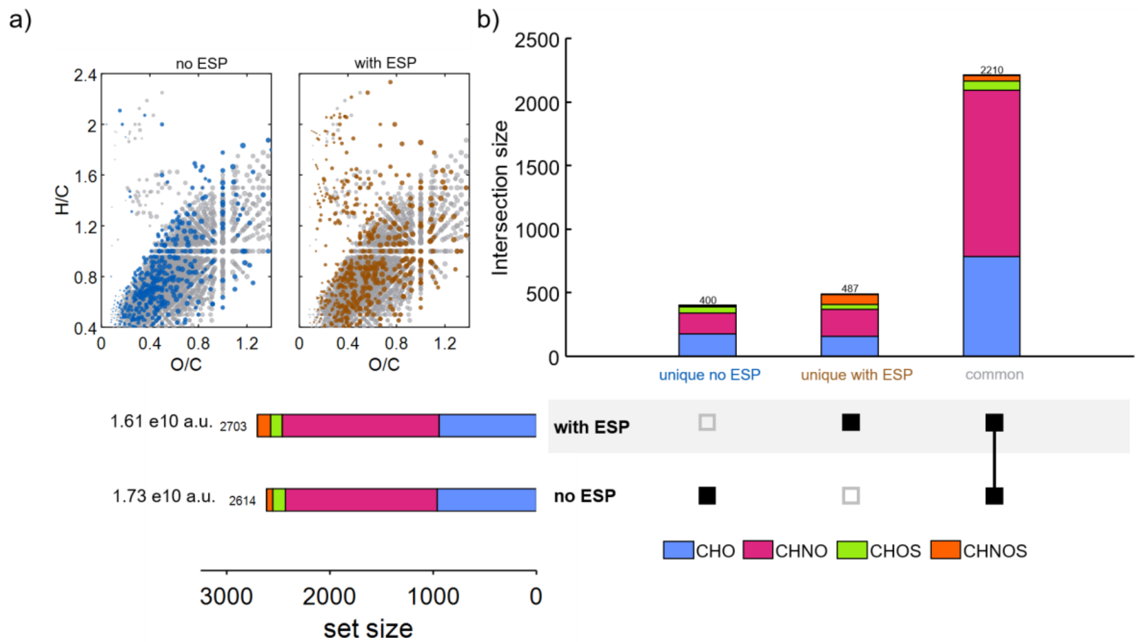

Figure S9: Upset plot of short aged wood combustion emissions (ESI-) with and without application of an electrostatic precipitator (ESP) showing unique and common elemental compositions of the two experiments. Van Krevelen diagrams (top left) showing the distribution of compounds found only in the short aging emissions without ESP (blue), with ESP (brown), or in both (grey). TIC (set size) is indicated in brackets behind the respective number of compounds in each dataset.

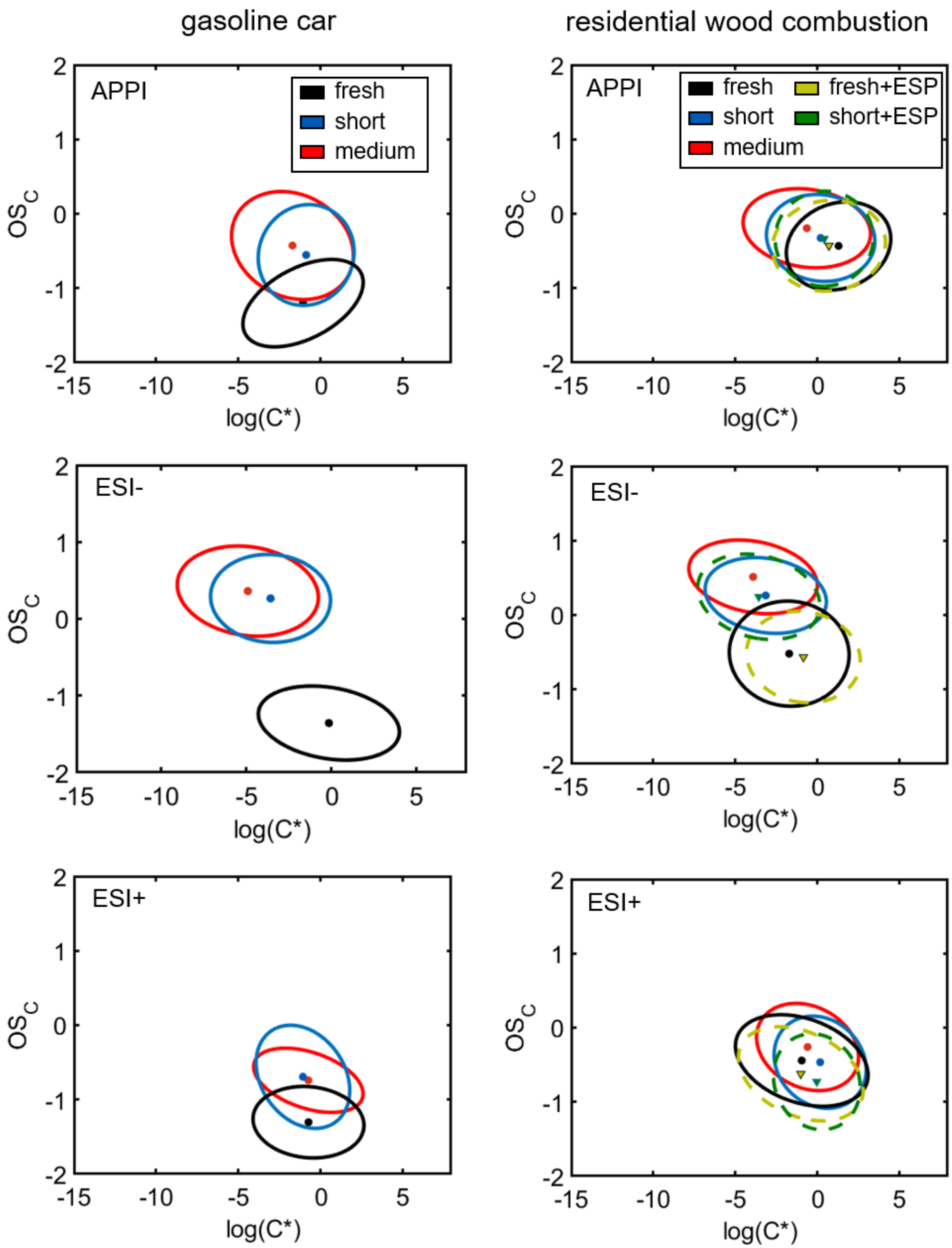

Figure S10: Average carbon oxidation state (OS_C) versus saturation vapor pressure (log(C*)) plots of gasoline car (right) and residential wood combustion (right) emissions separated by ionization method, with intensity weighted mean values (dots) and ellipses indicating the 50% confidence interval of the log(C*) versus OS_C distribution. Fresh emissions are indicated in black, short aged in blue and medium aged in red. Fresh and short aged wood combustion emissions with application of an electrostatic precipitator (ESP) are indicated by triangles (green) with dotted lines indicating the respective confidence interval.

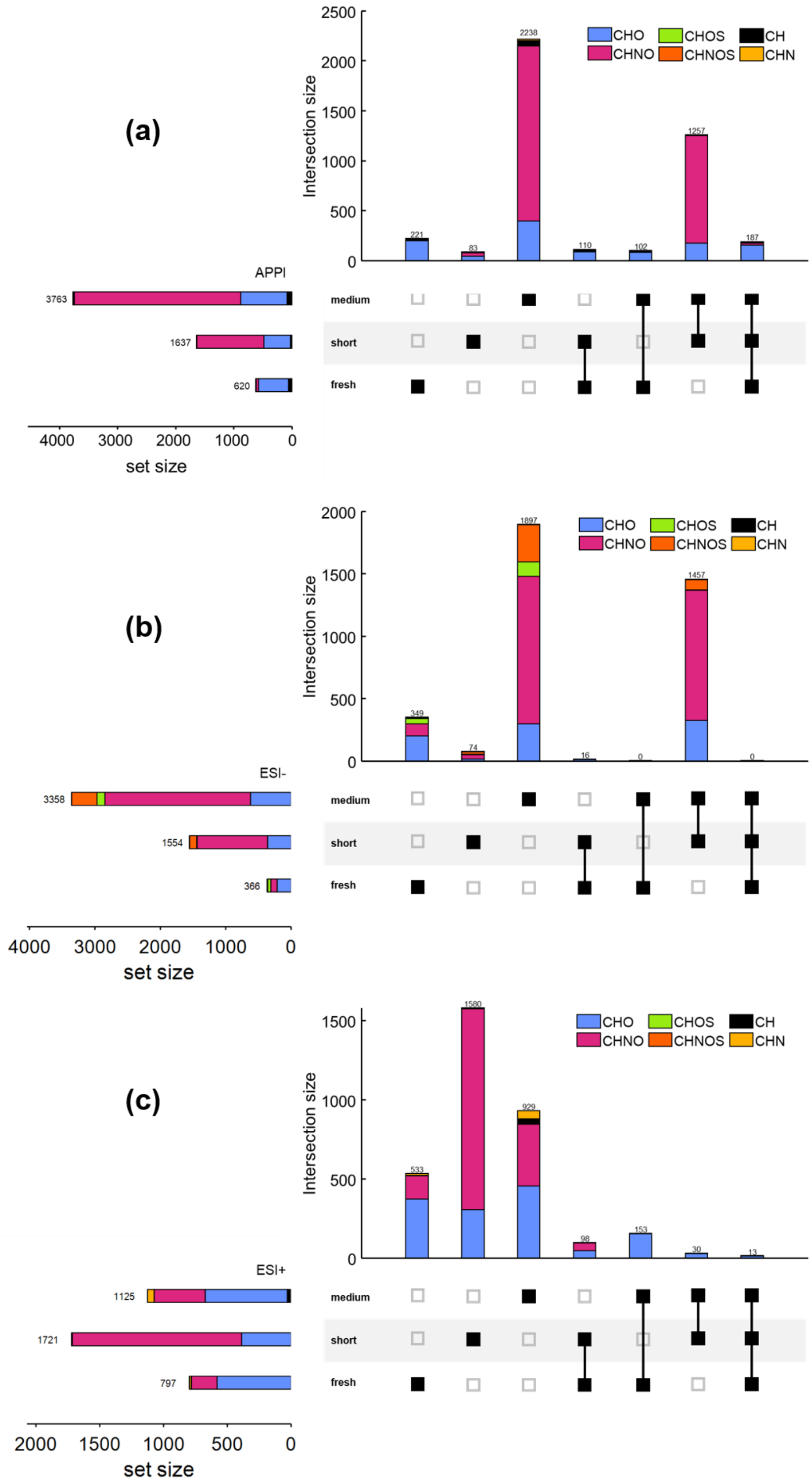

Figure S11: Upset plots of assigned elemental compositions from fresh, short aged and medium aged gasoline car emissions with indicated compound class, detected in **(a)** APPI **(b)** ESI- and **(c)** ESI+. TIC (set size) is indicated in brackets behind the respective number of compounds in each dataset.

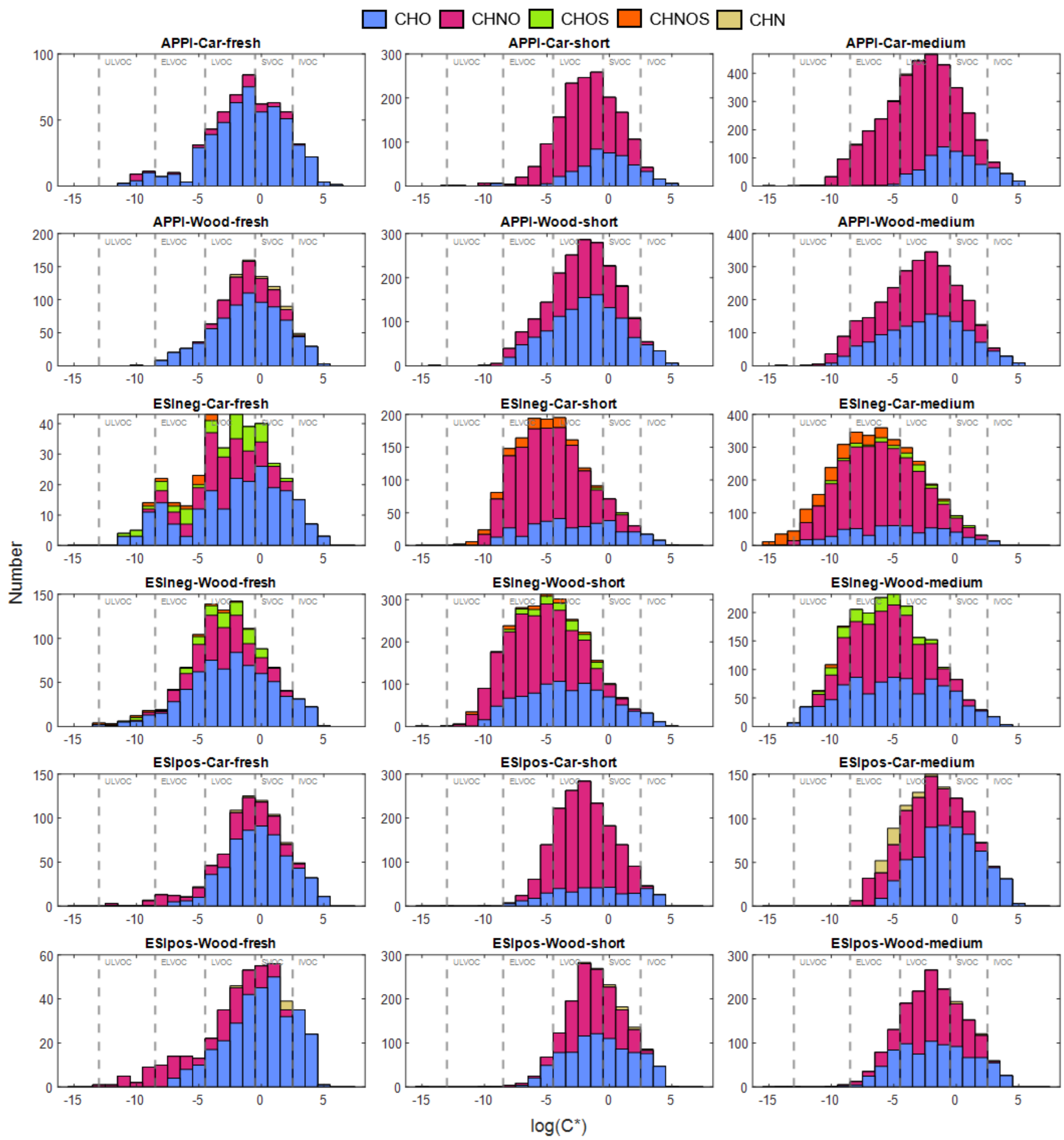

Figure S12: Distribution of compound classes (number) in separated volatility bins (log(C*)) for each ionization technique, emission source and intensity of photochemical aging. Organic compound volatility ranges of intermediate volatile (IVOC), semi volatile (SVOC), low-volatile (LVOC) extremely-low volatile (ELVOC) and ultra-low volatile (ULVOC) are indicated by dotted vertical lines.

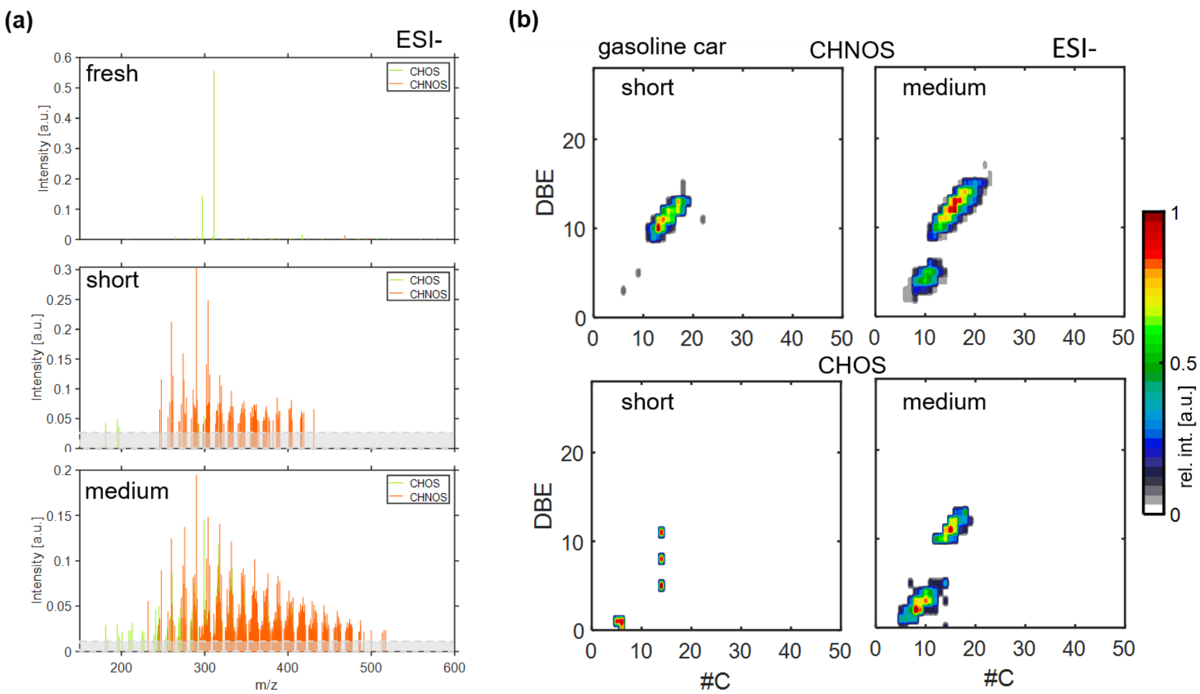

Figure S13: (a) Mass spectra (ESI-) of assigned sulfur-containing elemental compositions (CHOS: green, CHNOS: orange) in fresh, short aged and medium aged gasoline car emissions. The grey area indicates the signal-to-noise threshold for peak picking. **(b)** Contour plot of double bond equivalent (DBE) versus carbon number plot of the CHNOS (top) and CHOS (bottom) compound class in short and medium aged ESI(-) data of gasoline car emissions.

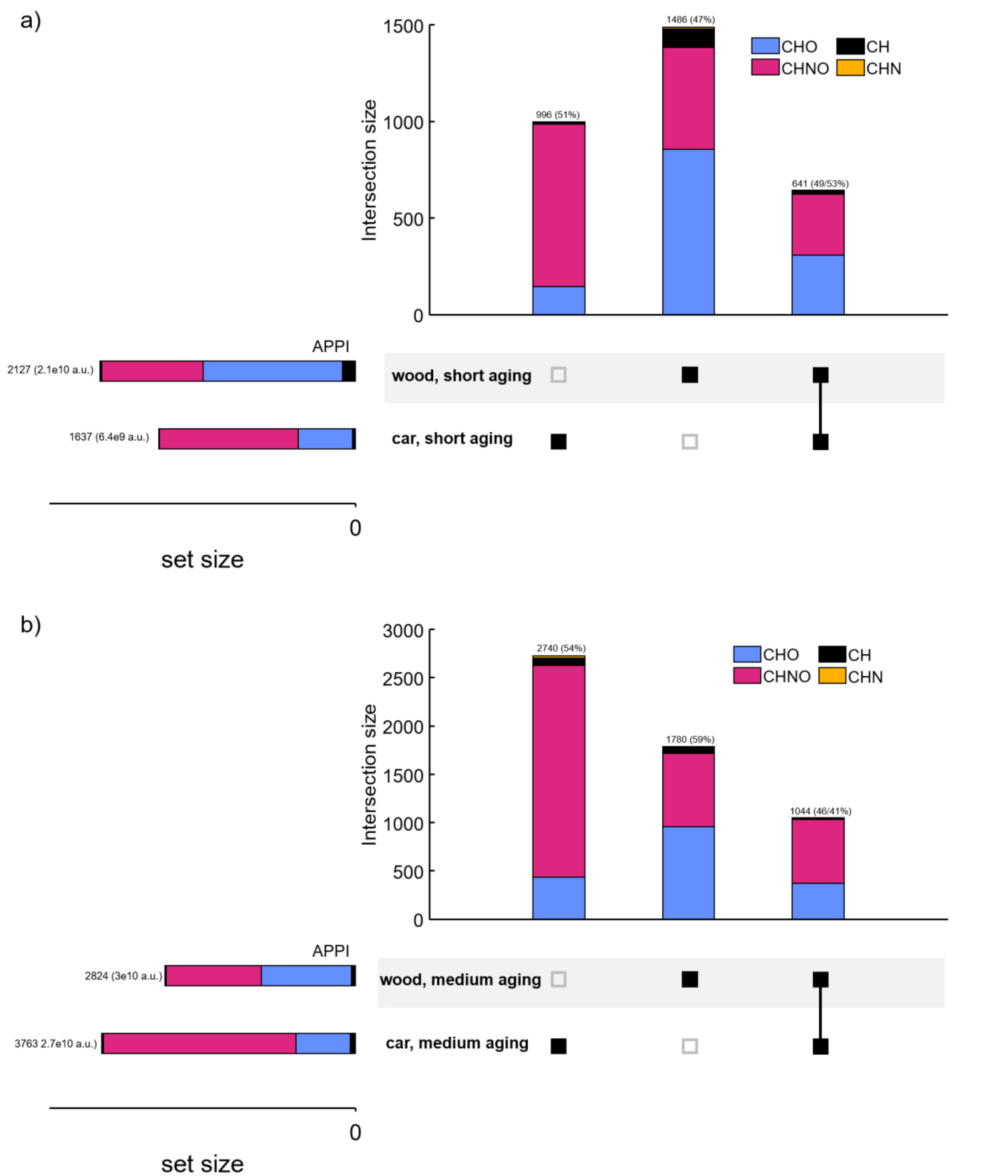

Figure S14: Upset plots of the comparison of gasoline car and residential wood combustion emission aging after **a)** short and **b)** medium aging. Relative compound class number distribution indicated by color. TIC (set size) or relative intensity (intersection size) is indicated in brackets behind the respective number of compounds in each intersection or the total number of compounds in each dataset.

References

1 J. H. Kroll, N. M. Donahue, J. L. Jimenez, S. H. Kessler, M. R. Canagaratna, K. R. Wilson, K. E. Altieri, L. R. Mazzoleni, A. S. Wozniak, H. Bluhm, E. R. Mysak, J. D. Smith, C. E. Kolb and D. R. Worsnop, Carbon oxidation state as a metric for describing the chemistry of atmospheric organic aerosol, *Nat. Chem.*, 2011, **3**, 133–139.

2 B. P. Koch and T. Dittmar, From mass to structure: an aromaticity index for high-resolution mass data of natural organic matter, *Rapid Commun. Mass Spectrom.*, 2006, **20**, 926–932.

3 Y. Li, U. Pöschl and M. Shiraiwa, Molecular corridors and parameterizations of volatility in the chemical evolution of organic aerosols, *Atmos. Chem. Phys.*, 2016, **16**, 3327–3344.

4 Y. Li, U. Pöschl and M. Shiraiwa, Molecular corridors and parameterizations of volatility in the chemical evolution of organic aerosols, *Atmos. Chem. Phys.*, 2016, **16**, 3327–3344.

5 N. M. Donahue, S. A. Epstein, S. N. Pandis and A. L. Robinson, A two-dimensional volatility basis set: 1. organic-aerosol mixing thermodynamics, *Atmos. Chem. Phys.*, 2011, **11**, 3303–3318.

6 Z. Peng and J. L. Jimenez, Modeling of the chemistry in oxidation flow reactors with high initial NO, *Atmos. Chem. Phys.*, 2017, **17**, 11991–12010.

7 A. Hartikainen, P. Tiitta, M. Ihalainen, P. Yli-Pirilä, J. Orasche, H. Czech, M. Kortelainen, H. Lamberg, H. Suhonen, H. Koponen, L. Hao, R. Zimmermann, J. Jokiniemi, J. Tissari and O. Sippula, Photochemical transformation of residential wood combustion emissions: dependence of organic aerosol composition on OH exposure, *Atmos. Chem. Phys.*, 2020, **20**, 6357–6378.

8 B. B. Palm, P. Campuzano-Jost, A. M. Ortega, D. A. Day, L. Kaser, W. Jud, T. Karl, A. Hansel, J. F. Hunter, E. S. Cross, J. H. Kroll, Z. Peng, W. H. Brune and J. L. Jimenez, In situ secondary organic aerosol formation from ambient pine forest air using an oxidation flow reactor, *Atmos. Chem. Phys.*, 2016, **16**, 2943–2970.